Convolutional Neural Networks Using Dynamic Functional Connectivity for EEG-Based Person Identification in Diverse Human States

Min Wang, *Student Member, IEEE*, Heba El-Fiqi, *Member, IEEE*, Jiankun Hu, *Senior Member, IEEE*, and Hussein A. Abbass, *Senior Member, IEEE*

***Abstract*— Highly secure access control requires Swiss-cheese-type multi-layer security protocols. The use of electroencephalogram (EEG) to provide cognitive indicators for human workload and fatigue has created environments where the EEG data are well-integrated into systems, making it readily available for more forms of innovative uses including biometrics. However, most of the existing studies on EEG biometrics rely on resting state signals or require specific and repetitive sensory stimulation, limiting their uses in naturalistic settings. Moreover, the limited discriminatory power of uni-variate measures denies an opportunity to use dependences information inherent in brain regions to design more robust biometric identifiers. In this paper, we proposed a novel model for ongoing EEG biometric identification using EEG collected during a diverse set of tasks. The novelty lies in representing EEG signals as a graph based on within-frequency and cross-frequency functional connectivity estimates, and the use of graph convolutional neural network (GCNN) to automatically capture deep intrinsic structural representations from the EEG graphs for person identification. An extensive investigation was carried out to assess the robustness of the method against diverse human states, including resting states under eye-open and eye-closed conditions and active states drawn during the performance of four different tasks. We compared our method with the state-of-the-art EEG features, classifiers, and models of EEG biometrics. Results show that the representation drawn from EEG functional connectivity graphs demonstrates more robust biometric traits than direct use of uni-variate features. Moreover, the GCNN can effectively and efficiently capture discriminative traits, thus generalizing better over diverse human states.**

***Index Terms*— EEG, biometrics, person identification, functional connectivity, convolutional neural network, deep learning.**

I. Introduction

CONFIRMING human identity is becoming more critical in the vastly interconnected society, leading to increasing needs for reliable user identification techniques to meet the wake of heightened security. This is becoming especially important in highly secure operations such as air traffic control, which extends to space operations, and supervisory control or teleoperations of autonomous systems including teleoperations of unmanned aerial vehicles (UAVs). In these sophisticated environments, there is an extensive literature exploring the use of electroencephalogram (EEG) to provide real-time human workload and fatigue indicators to dynamically adapt the environment to human cognitive states [1]. These environments have EEG data readily available, opening more opportunities for their use as a security layer for biometrics.

EEG measures electrical potentials generated from neural activities at the scalp level by portable and non-invasive devices [2], [3]. It provides the most promising bio-signals for automatic person identification due to its rich dynamics and high temporal resolution [4]. Compared with conventional identification techniques that rely on passwords, fingerprints, facial and retinal scans, EEG potentially provides superior biometrics when considering the following five distinguished features [4]–[6].

- Fingerprints or facial images can be elaborately forged or secretly duplicated via high resolution photographs. EEG signals during a task that naturally requires conscious engagement of a human subject cannot be captured without the person's awareness. This affords EEG with a unique anti-forgery capacity.
- EEG is bidirectional hack-proofed. The high security level of EEG biometrics is also guaranteed from the user side as many features of EEG are non-volitional (not under control or conscious apprehensions of the user), which means that the user cannot deliberately divulge their identifiers [7].
- As pointed out in previous research [7], brain activity provides an "alive biometrics" that a user must be alive in order to provide active signals. This characteristics can protect the users while protecting the system.
- As natural continuous biological signals, EEG can be used to design an unobtrusive continuous authentication

Manuscript received March 3, 2019; revised April 26, 2019; accepted April 30, 2019. Date of publication May 16, 2019; date of current version August 22, 2019. This work was supported by the Australian Research Council through the discovery grant DP160102037. The associate editor coordinating the review of this manuscript and approving it for publication was Dr. Andrew Beng Jin Teoh. *(Corresponding author: Jiankun Hu.)*

The authors are with the School of Engineering and Information Technology, University of New South Wales, Canberra, ACT 2612, Australia (e-mail: min.wang@student.adfa.edu.au; h.el-fiqi@adfa.edu.au; j.hu@adfa.edu.au; h.abbass@adfa.edu.au).

This article has supplementary downloadable material available at http://ieeexplore.ieee.org., provided by the authors. The material includes the results of the statistical significance test of the correct recognition rate results. Contact min.wang@student.adfa.edu.au for further questions about this work.

Digital Object Identifier 10.1109/TIFS.2019.2916403

system which is important in critical applications where interruption could potentially result in hazardous consequences.
- EEG biometrics also provides cognitive information that can be used for cognitive load estimation and fatigue detection [1].

Although EEG provides a contested complement to existing biometric modalities, research on EEG-based person identification is still in its early stage. Visual evoked potential (VEP) and event-related potential (ERP) paradigms have been designed to elicit specific brain responses for user recognition purpose, achieving a correct recognition rate (CRR) of above 95% by combining resultant responses from multiple stimuli [7], [8]. However, this type of methods relies on elaborate EEG elicitation paradigms and repetitive sensory stimulation, thereby, their applications in naturalistic settings are limited.

To avoid repetitive sensory stimulation to better fit the naturalistic settings, ongoing EEG in resting state is studied [9]. Resting state is an advantageous condition for EEG biometrics as the signals are not affected by active involvement of the subjects. However, the resting state alone is not sufficient for practical uses because there is no guarantee that the user state will remain in the resting state. In practical applications, it is necessary to relax the restrictions on state, task and signal elicitation paradigms, and to design a method for person identification in diverse human states. The issue of task sensitivity of EEG biometrics is discussed in a recent study [10]. However, only motor imagery tasks are used in the analysis due to the limitation of available databases.

In this paper, we focus on biometric identification using ongoing EEG signals in diverse human states. A comprehensive study is carried out using two datasets, spanning six different human states to extend the current analysis in more diverse human states. A learning model based on functional connectivity and graph convolutional neural network (GCNN) is proposed. In particular, we propose a graph representation method for EEG signals based on within-frequency and cross-frequency functional connectivity towards deep learning. In addition, a GCNN-based deep learning module is designed to automatically capture important features in the dynamic functional connectivity graphs (FCG) generated in the graphical representation module. In practical deployment of EEG biometric systems, a method that can generalize over diverse human states has significant advantages over methods that require specific states, tasks, or signal elicitation paradigms.

This paper contributes to the literature on EEG-based person identification in two folds. The first is the proposed learning model that generates graph representations of EEG signals and automatically extracts deep structural features from dynamic EEG graphs for person identification. The graph representation addresses the problems associated with methods relying on uni-variate features by using functional couplings between signals. It also facilitates the use of GCNN to extract intrinsic structural features, which potentially leads to better performance and higher capacity to generalize over diverse human states. The second contribution is a comprehensive investigation of the proposed method and comparison methods using EEG signals of diverse human states. It can be regarded as an extension and supplement to research on the permanence [11] and task sensitivity [10] of EEG biometrics.

The remainder of this paper is structured as follows. Section II reviews the state of art research on EEG biometrics. Section III presents the proposed methodology. Section IV describes the experimental design, followed by results in Section V and discussion in Section VI. Finally, Section VII concludes this study and indicates potential future work.

II. Previous Work on EEG for Biometrics

In this section, we review relevant literature on state-of-the-art methods for EEG biometrics. Since the contributions of this paper lie in improving the applicability of, and proposing a learning model for, EEG-based identification methods, the existing literature is reviewed from three perspectives, namely tasks and states, features, and classifiers.

A. Tasks and States

A paradigm based on event-related potentials (ERP), named Brainprint [12], was proposed for brain biometrics using semantic memory. A single-word reading protocol was designed to trigger the N400 response resultant from an individual's semantic memory. Another ERP protocol named 'CEREBRE' [7] extended the Brainprint system by including different types of stimuli (e.g., images of food, celebrities, words, etc.) to elicit multiple reactions. An identification accuracy of 100% was achieved by integrating these reactions from multiple categories of stimuli. P300, which is ERP that get triggered by rare events, was also exploited for biometrics [13]. In addition to the ERP school, another school of thoughts relying on visual evoked potentials (VEP) was proposed for person identification [8], [14], [15]. For example, steady-state VEP signals triggered by a flickering grid-shaped visual array were used in a recent study [8]. The design of the visual array was based on Korean letters, therefore it would be difficult for people from other cultures to use it. A maximal accuracy of 98.60% was achieved in identifying 20 subjects with EEG causal connectivity in 16 brain regions. Methods based on ERP and VEP signals suffer a common defect that their practicality is relatively low since ERP and VEP are essentially averaged signals over signals of multiple trials and these signals are time-locked to some stimulation of interest. Specifically, the underlying process of triggering the neural responses within ERP or SSVEP based protocols requires repetitive presentation of the stimuli in highly controlled conditions, limiting their practical application.

Ongoing EEG signals collected in the absence of any particular stimulation provide a better solution for real-world applications. Resting states ongoing EEG signals have been investigated in many studies [16]–[18] which achieved an identification accuracy ranging from 72% to 95% on a sample pool of less than 40 subjects with different EEG channels, features and classifiers. It is an advantageous condition, however, not sufficient for real-world scenarios where the human states are changing and cannot be guaranteed to be constantly resting. The identification system should also be able to work

properly while the users are performing mental or physical tasks, of which the EEG signals are called active ongoing EEG. Active ongoing EEG signals suffer from the effects associated with continuously changing human states, including physical ones such as movements and artifacts, and psychological ones such as cognitive workload, fatigue and emotion. Therefore, it is a big challenge to design proper algorithms that can learn robust biometric traits from EEG dynamics and can generalize over diverse human states.

A recent study explores the sensitivity of EEG biometrics to the type of tasks by applying different training and testing strategies [10]. Our work extends their analysis by including more diverse human states. More importantly, we discussed some critical, however neglected, issues of EEG-based identification systems, such as adding new users to the system, and rejecting unregistered users, which represent important supplements to existing study on issues pertinent to the usability of EEG biometrics [19].

B. Features

Most methods for EEG-based person identification rely on features extracted from signals of single electrodes corresponding to different brain regions. Widely-used features include coefficients of auto-regressive (AR) stochastic models [16]–[18], power spectral density (PSD) functions [14], [20], [21] and entropy measures (e.g., fuzzy entropy) which estimate signal complexity [20], [22]. Features based on wavelet transform [10] and Hilbert-Huang transform [23] were also proposed for EEG biometrics recently. However, uni-variate features only capture characteristics of signals from single electrodes, neglecting the interconnection information between signals from different electrodes. More importantly, uni-variate features can be easily affected by the changes of EEG amplitudes which are caused by inevitable physiologic or psychological factors such as circadian rhythms [24], different signal acquisition solutions or simply recording conditions [25].

In general, functional connectivity captures deviations from statistical independence between distributed and spatially separated neuronal units. It is a bi-variate measure that captures the coupling relation of two signals, making it less sensitive to the EEG amplitude changes. This property could reduce EEG intra-person variation, which is a critical aspect in improving the overall performance of EEG-based person recognition systems.

Functional connectivity was first introduced in EEG biometrics by A. Riera in 2008 [16]. In that study, time-domain connectivity between signals from two frontal electrodes was used for identification of 51 subjects, achieving a CRR of 31% using cross-correlation. Spectral coherence (COH), a frequency-domain connectivity measure, was investigated for human distinctiveness by D.La Rocca in 2014 [9]. A CRR of 100% was achieved on identifying 108 subjects with a match-score fusion of the COH features. However, this study suffered the problem of very small sample size (only 5 samples per subject for training and 1 for testing), which might lead to unreliable results. Phase lag index (PLI) and phase locking value (PLV) were tested for subject verification and identification, respectively [26], [27]. Results indicated that phase synchronization measures could provide more stable functional connectivity estimates than time-domain measures. In addition to functional connectivity, effective connectivity (e.g., Granger causality) was used in a VEP-based biometric system [8]. Despite of positive results, some limitations remain including the small number of subjects (e.g., 9 in [27]), the dependence on resting states alone (e.g., [9], [26]), and the complexity of proposed signal elicitation procedures (e.g., the method proposed in [8] relies on a Korean character-based steady-state VEP paradigm which requires subjects receiving multiple visual stimuli repetitively in a controlled environment). In addition to using functional connectivity values directly as feature vectors (as in the above-mentioned research), other studies have focused on extracting topological features (node degrees [27] and eigenvector centrality [26]) of networks generated by functional connectivity. However, a common disadvantage of these methods is that they do not fully exploit the inherent structural information of the functional connectivity networks which could be important in improving performance.

C. Classifiers

Current research on EEG biometrics mainly applies conventional classifiers such as support vector machines (SVM), K-nearest neighbors (kNN), Multi-Layer Perceptrons (MLP) and distanced-based classifiers [9], [14], [20], [22]. These classifiers usually achieve good results when the classification boundary is relatively clear. This requires the designed feature set to be highly effective and remain discriminative over time, which is a problem in EEG of different states due to the rich dynamics and time-varying characteristics. Domain knowledge can help design effective features, however, it cannot guarantee that these features have enough discriminative power during different cognitive states.

Deep learning provides a solution to the above problem. It has been supported by theoretical results and empirical evidences that a deep, hierarchical model can extract deeper and more significant representations from the input in comparison with conventional classifiers [28], [29]. Convolutional neural networks (CNN) have been used for EEG biometric identification [30]–[35] and verification [31], [36], [37] in recent studies, as summarized in Table I. In these studies, CNN is directly used to learn representations from the amplitudes of the EEG timeseries which, however, change in different human states, making the learnt representations sensitive to human states. This is partially the reason why these studies require ERP/VEP signals (which are collected in tightly controlled conditions) or resting-state EEG signals (which are free from active involvement of the subjects). The method proposed in this paper has similar motivation to the above methods, that is, to make use of the powerful learning ability of CNN. However, what differs from the above methods is that we aim to learn intrinsic and robust structural features, rather than features based on signal amplitudes. As we mentioned in Section II.B, there is an intrinsic relationship between EEG signals from

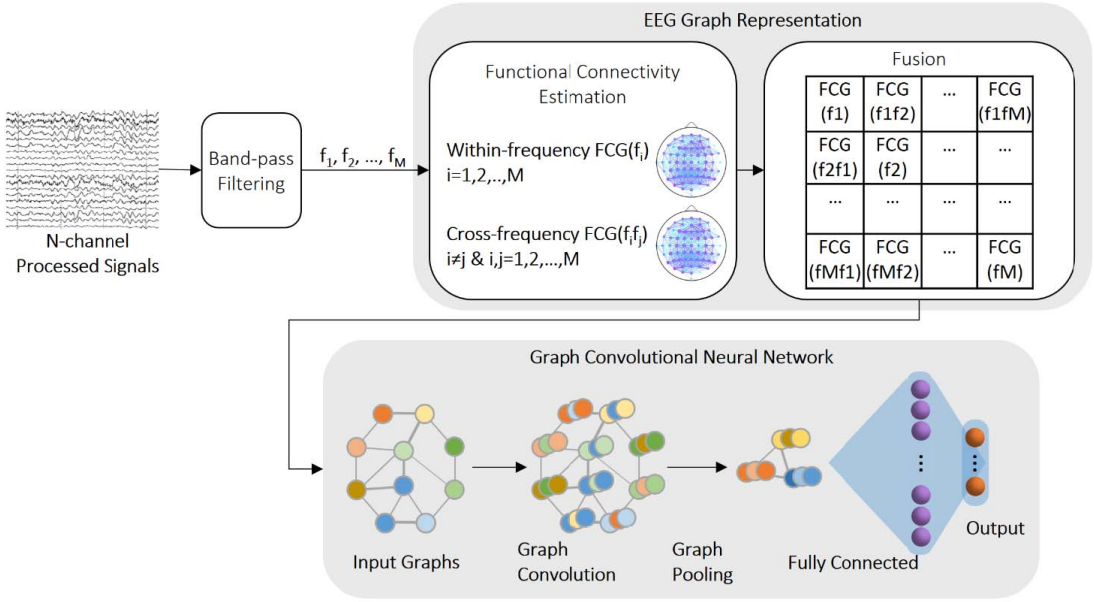

Fig. 1. Proposed learning model.

TABLE I
EEG BIOMETRICS USING CNN. CRR-CORRECT RECOGNITION RATE, EER-EQUAL ERROR RATE, ACC-ACCURACY

Ref	Scenarios	Inputs	#Subjects	Results
[30]	Identification	VEPs	40	97.9% (CRR)
[31]	Identification	VEPs	10	95.9% (CRR)
[32]	Identification	EEG	100	97% (CRR)
[33]	Identification	EEG(resting)	40	99.2% (CRR)
[34]	Identification	EEG(resting)	10	82% (CRR)
[36]	Verification	EEG(resting)	109	0.19% (EER)
[37]	Verification	VEP features	40	92.4% (ACC)

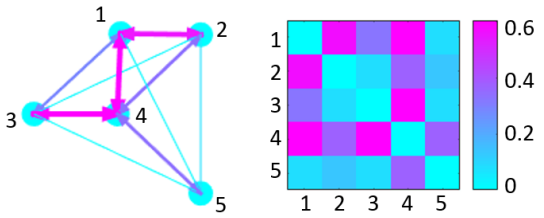

Fig. 2. A simple undirected and weighted graph with five nodes (left) and its corresponding adjacency matrix.

different electrodes (regions), i.e., functional connectivity, which exhibits individual distinctiveness. We conjecture that the structural representations learnt from FCGs could provide more robust human distinctiveness in different states. In order to do that, we propose a graph representation approach to present the intrinsic structural characteristics of EEG signals, and use a GCNN model to learn deep abstracts from the graphs for person identification. The design of the GCNN is motivated by a recent work by M. Defferrard [38] which aims to extend CNN to graph domain with graph theory.

III. METHODOLOGY

In this section, we present the proposed model of learning biometric traits from EEG for person identification which, as illustrated in Fig. 1, consists of two main components: a graph generation component to obtain rich graph representation of EEG signals; and a classification component based on GCNN to learn discriminative patterns from EEG graphs estimated from the first component.

EEG signals are typically described in terms of rhythmic activities in the following five frequency bands: delta (0-4Hz), theta (4-7Hz), alpha (8-13Hz), beta (13-30Hz), and gamma (30-42Hz). Therefore, band-pass filtering is applied before calculating functional connectivity to decompose the pre-processed multi-channel EEG signals into sub-band signals. The graph representation component takes these sub-band EEG signals as inputs and generates graphs which describe the within-frequency and cross-frequency functional connectivity between signals from any two electrodes. Finally, the generated EEG graphs are fed into a GCNN for graph feature extraction and classification.

A. Network and Graph

An undirected and connected network graph can be defined by a set of nodes ($\mathcal{V}$) and a set of edges ($\mathcal{E}$) that connect these nodes, as $\mathcal{G} = \{\mathcal{V}, \mathcal{E}\}$, in which $N = |\mathcal{V}|$ denotes the number of nodes in the graph. The edges between nodes $\mathcal{E}$ can be formulated as an adjacency matrix $\mathbf{A} \in \mathbb{R}^{N \times N}$ which is a representative description of the graph structure. The entry of the adjacency matrix, denoted as $a_{i,j}$, represents the importance of the connection between node i and node j. Fig. 2 illustrates a simple network graph with five nodes and its corresponding adjacency matrix.

B. Graph Representation of EEG Signals

The graph representation component converts a multi-electrode EEG signal into an FCG, where the weight of each edge is defined by PLV.

TABLE II
FUNCTIONAL CONNECTIVITY

Methods	Range	Description	Computing time
COR	$[-1, 1]$	Time-domain linear correlation	34.8 ms
PLV	$[0, 1]$	Variability of relative phase	87.0 ms

Let $s_i^{f_p}(t)$ denote EEG signal from electrode i associated with frequency band f_p. The PLV of two signals, $s_i^{f_p}(t)$ and $s_j^{f_q}(t)$, is defined in Equation (1).

$$PLV(s_i^{f_p}, s_j^{f_q}) = \left|\left\langle e^{im\triangle\phi_r(t)}\right\rangle\right| \tag{1}$$

$$= \left|\frac{1}{N_s}\sum_{k=1}^{N_s} e^{im(\phi_i(k)-\phi_j(k))}\right| \tag{2}$$

where $\Delta\phi_r(t)$ is the relative phase, defined as $\Delta\phi_r(t) = |\phi_{s_i}(t) - \phi_{s_j}(t)| \mod 2\pi$, in which $\phi_s(t)$ is the instantaneous phase of a signal and is calculated by applying Hilbert transform to the original signal $s^f(t)$.

PLV measures the average difference between the instantaneous phases of two signals over time on the unit circle. The range of PLV values is $[0, 1]$, where 0 refers to the absence of phase coupling (uniform distribution of $\Delta\phi_r(t)$) and 1 indicates strict phase coupling (Dirac distributed). PLV is an effective tool to measure the coordinated activation over different brain regions in EEG domain [39]. It provides an indication of short-range perceptual binding among adjacent brain regions as well as long-range synchronization patterns between more widely separated brain regions. Since EEG signals are essentially composed by a series of rhythmic oscillations, we conjecture that PLV would lead to more robust connectivity estimates than time-domain measures. To validate this hypothesis, Pearson's correlation (COR), as defined in Equation (3), is also evaluated in our investigation.

$$COR(s_i^{f_p}, s_j^{f_q}) = \frac{1}{N_s}\sum_{k=1}^{N_s} s_i^{f_p}(k)s_j^{f_q}(k) \tag{3}$$

Table II summarizes the two types of functional connectivity and the corresponding computing time of generating an FCG using 64-electrode EEG signals. Both of them are time-friendly, therefore are suitable for practical applications.

The within-frequency FCG is generated by calculating PLV (or COR) for every two electrodes using signals in the same frequency band ($p = q$), and the cross-frequency FCG is generated by calculating PLV (or COR) for every two electrodes (including each electrode and itself) using signals in different frequency bands ($p \neq q$). Finally the adjacency matrices of the M within-frequency FCGs and $M(M-1)$ cross-frequency FCGs are fused into an extended EEG graph representation which has $N \times M$ nodes, as illustrated in Fig. 1, where N and M denote the number of electrodes and the number of frequency bands, respectively.

C. Graph Convolutional Neural Network

The design of graph convolutional filters is the major problem in generalizing the classical CNN to handle graph inputs. Spectral filters in Fourier domain based on the spectral graph theory are elegant solutions [40]. For a graph $\mathcal{G}$, its graph Laplacian $\mathbf{L}$ is defined as:

$$\mathbf{L} = \mathbf{D} - \mathbf{A} \in \mathbb{R}^{N\times N} \tag{4}$$

$$\mathbf{L} = \mathbf{I}_N - \mathbf{D}^{-1/2}\mathbf{A}\mathbf{D}^{-1/2} \quad \texttt{(normalized)}, \tag{5}$$

where $\mathbf{I}_N$ is an identity matrix, and $\mathbf{D} \in \mathbb{R}^{N\times N}$ is the diagonal degree matrix, each element of which is the sum of each corresponding row as $D_{ii} = \sum_j a_{ij}$.

For a graph signal $\mathbf{x} \in \mathbb{R}^N$, its graph Fourier transform is defined as:

$$\hat{\mathbf{x}} = \mathbf{U}^T\mathbf{x}, \quad \mathbf{x} = \mathbf{U}\hat{\mathbf{x}} \quad \texttt{(inverse)}, \tag{6}$$

in which $\mathbf{U} = [\mathbf{u_0}, ..., \mathbf{u}_{N-1}] \in \mathbb{R}^{N\times N}$ is the Fourier basis that calculated by eigenvector decomposition of $\mathbf{L}$, namely $\mathbf{L} = \mathbf{U}\Lambda\mathbf{U}^T$. The associated eigenvalues $\Lambda = \texttt{diag}([\lambda_0, ..., \lambda_{N-1}]) \in \mathbb{R}^{N\times N}$ are regarded as the graph frequencies.

For two graph signals $\mathbf{x}$ and $\mathbf{y}$, their convolution on graph $*\mathcal{G}$ is then expressed as:

$$\mathbf{x} * \mathcal{G}\mathbf{y} = \mathbf{U}((\mathbf{U}^T\mathbf{x}) \odot (\mathbf{U}^T\mathbf{y})), \tag{7}$$

where $\odot$ represents the element-wise Hadamard product.

Now let g_θ denotes the filter with parameter θ, the filtering process of signal $\mathbf{x}$ can be written as:

$$\mathbf{y} = g_\theta(\mathbf{L})\mathbf{x} = g_\theta(\mathbf{U}\Lambda\mathbf{U}^T)\mathbf{x} = \mathbf{U}g_\theta(\Lambda)\mathbf{U}^T\mathbf{x}, \tag{8}$$

where $g_\theta(\Lambda) = \texttt{diag}([g_\theta(\lambda_0), ..., g_\theta(\lambda_{N-1})])$ is the graph filter. Directly learning the filters $g_\theta(\Lambda)$ in spectral domain requires to solve the graph Laplacian eigenbasis, which transforms a graph between spatial and spectral domains. Since the eigenbasis is unique for each graph structure, the input samples need to be homogeneous, otherwise we need to solve eigenbasis for each different graph. To solve this problem, the filer is polynomially parameterized as linear combinations of K-order Chebyshev [38], as:

$$g_\theta(\Lambda) = \sum_{k=0}^{K-1}\theta_k T_k(\tilde{\Lambda}), \tag{9}$$

in which $\theta \in \mathbb{R}^K$ denotes the coefficient vector of the Chebyshev polynomials, $\tilde{\Lambda} = 2\Lambda/\lambda_{max} - \mathbf{I}_N$ denotes the scaled eigenvalues, $T_k(x)$ denotes the Chebyshev polynomial of order k and can be recursively computed according to the recurrence relation: $T_k(x) = 2xT_{k-1}(x) - T_{k-2}(x)$ with $T_0(x) = 1$ and $T_1(x) = x$.

Finally, the graph convolution formulated in (8) can be rewritten as:

$$\mathbf{y} = \mathbf{U}g_\theta(\Lambda)\mathbf{U}^T\mathbf{x} \tag{10}$$

$$= \sum_{k=0}^{K-1}\theta_k\mathbf{U}T_k(\tilde{\Lambda})\mathbf{U}^T\mathbf{x} \tag{11}$$

$$= \sum_{k=0}^{K-1}\theta_k T_k(\tilde{\mathbf{L}})\mathbf{x}, \tag{12}$$

where $\tilde{\mathbf{L}}$ is scaled Laplacian: $\tilde{\mathbf{L}} = 2\mathbf{L}/\lambda_{max} - \mathbf{I}_N$. The above graph convolution allows the learnt weights to be shared across

TABLE III
CONFIGURATION OF THE GCNN

Layer	Configuration
Graph Convolution	32 filters of 8th-order
Graph Max-Pooling	size 2
Graph Convolution	64 filters of 8th-order
Graph Max-Pooling	size 2
Fully Connected	ReLU (128)
Output	Softmax (109)

TABLE IV
DESCRIPTION OF DATASET

Dataset	#Subject	#Electrode	State /Duration(s) /#Samples			
			EO	EC	PHY	IMA
I	109	64	60	60	120×6(trials)	120×6(trials)
			119	119	239×6(trials)	239×6(trials)
			EO	EC	ATT	IMG
II	59	46	60	60	120	120
			119	119	239	239

different locations of the graph by using the localized filters defined in Equation (9).

The configuration of the GCNN model implemented in this work is summarized in Table III. In graph convolution layer, each output represents a convoluted feature extracted by a learnt local filter plus a non-linear activation function (ReLU). While in graph max-pooling layer, each output represents a salient feature after reducing dimensionality. After cascading two graph convolution and max-pooling layers, a flatten dense layer is fully connected to all activation of the previous layer and followed by the output layer.

The network was trained by iterating categorical cross entropy loss, as in (13), using Adam optimizer [41] with an initial learning rate of 0.001.

$$Loss = -\sum_{o=1}^{B}\sum_{c=1}^{C} y_{o,c} log(p_{o,c}) \tag{13}$$

where C denotes the number of classes, y is a hot encoding for the correct class with $y_{o,c}$ equals to 1 when the class label c matches the actual class of the observation o, and $p_{o,c}$ represents the probability that observation o is predicted as class c. $B = 200$ is the batch size. Batch normalizations [42] was applied before the graph convolution layer and fully connected layer to speed up the training process. And a dropout of 0.25 was adopted after the two graph max-pooling layers and the fully connected layer to reduce possible over-fitting [43].

IV. EXPERIMENTAL DESIGN

A. Datasets and Pre-Processing

Two datasets are used to evaluate the proposed method: an online database PhysioNet BCI (dataset I) [44] and a self-collected dataset (dataset II). Dataset I includes EEG signals collected under four human states: resting state with eyes-open (EO), resting state with eyes-closed (EC), physical movement tasks (PHY) which require the subjects to open or close their fists or feet, and motor imagery tasks (IMA) which require the subjects to imagine doing the above movements without actual physical movement. In addition to resting states EO and EC, dataset II provides EEG signals collected during another two tasks: an attention task (ATT) and an image description task (IMG). The ATT requires the subject to recognize the red letter from a series of letters that appear one by one quickly in the middle of the screen, and in IMG, the subjects is asked to describe a picture shown on the screen and type down their narratives.

Regarding data collection, a BCI2000 system [45] with 64 electrodes is used for dataset I and a Cognionics HD72 dry EEG system with 46 electrodes is used for dataset II. The signal sampling rate is 160Hz and 250Hz for dataset I and II, respectively. Signals from both datasets were referenced to the mean of the signals recorded from the subject's ear lobes. For signal pre-processing, an FIR filter with Hamming window was implemented to restrict the available frequency range to [0.5 42]Hz after removing the DC offset (the linear trend), then artifacts were removed using independent component analysis (ICA) [46]. A moving window of one-second with 50% overlap was used for generating training and testing samples. Therefore, each sample is based on one-second EEG data with a shape of 64×160 in dataset I and 46×250 in dataset II. These samples were labeled with the corresponding subject IDs. Table IV summarizes the details of the two datasets used in our experiments.

B. Experiments

Three experiments are designed to simulate real-world EEG-based application scenarios in diverse states.

Experiment 1 – Training and Testing Within Each Human State: In this experiment, we train and test each method using EEG signals in single states. Both dataset I and II were used for testing, providing six different states: EC, EO, PHY, IMA, ATT, and IMG. A five-fold cross-validation scheme with shuffling was applied for evaluation.

Experiment 2 – Training on Resting States and Testing on Diverse States: Resting states are important conditions in EEG experiments as they are normally conducted as baseline tasks for calibration before main tasks. In real-life scenarios, sometimes the EEG signal resources are limited during the enrolment stage (e.g., only resting-state signals available) but we need the system to continue working under more complex conditions (e.g., performing tasks). In this experiment, we aim to assess whether these methods can cope with EEG signals in diverse states using representations learnt from signals in resting states (when EEG signals under resting states are the only resources for training the system). For dataset I, we train the methods on EC and EO data, and test them on PHY and IMA data, separately. Similarly for dataset II, we train the methods on EC and EO data, and test them on ATT and IMG data, separately. We run each test 5 times to reduce bias in identification accuracy.

Experiment 3 – Training on Diverse States and Testing on Diverse States: The intra-person variation of EEG biometrics is considerable, which means a system trained with signals in one state may not work with signals in a different state. One way to address this problem is to train the model with signals of diverse states in order to force the model to cope

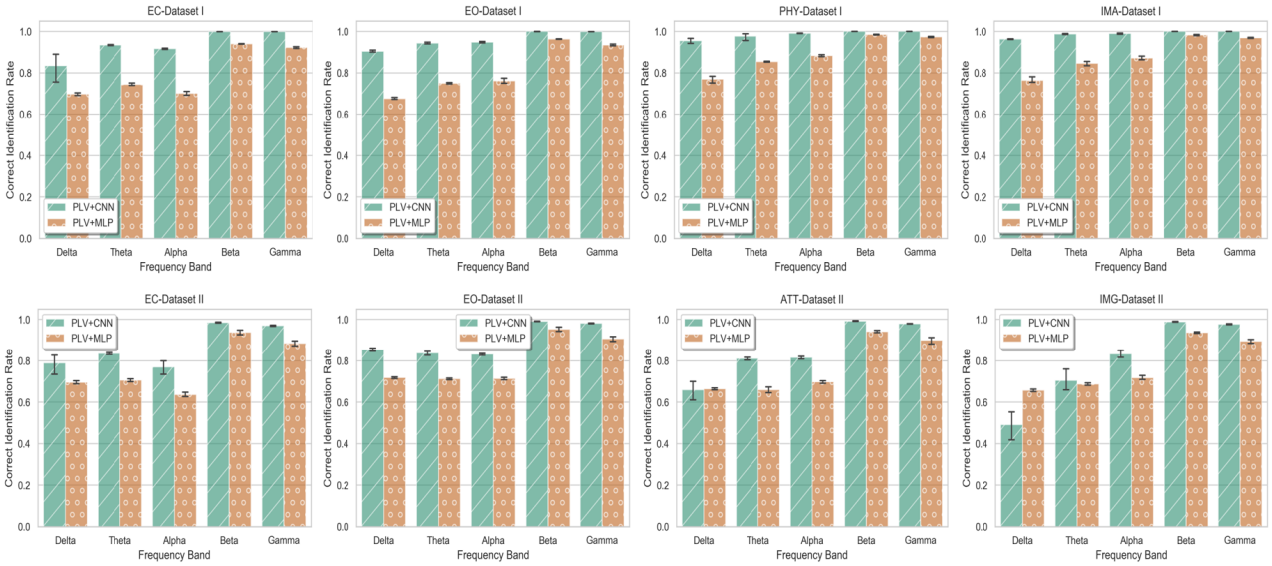

Fig. 3. Performance of PLV+GCNN and PLV+MLP for identifying 109 subjects in dataset I and 59 subjects in dataset II using EEG signals in the five canonical frequency bands. Results are CRR in testing stage.

with the intra-person variations. In this experiment, we mix the signals in different states for training and testing each method. A five-fold cross-validation scheme with shuffling was applied to evaluate the performance.

V. Results

State-of-the-art methods on EEG-based person identification mostly apply a procedure which comprises of hand-crafted features and traditional shallow classifiers. In our experiments, we selected three popular features: auto-regressive coefficient (AR), power spectral density (PSD), and fuzzy entropy (FuzzEn); and three classical classifiers: multi-layer perception (MLP), support vector machine (SVM), and random forest (RF). All the combinations of the above classifiers and features (or a combination of them) were evaluated. Furthermore, we also investigated CNN with raw EEG time-series inputs, denoted as 'Raw+CNN', and CNN with a combination of the uni-variant features, denoted as 'PSD+AR+FuzzEn+CNN'. Finally, we compared the proposed method 'PLV/COR+GCNN' with 'PLV/COR+CNN', wherein the latter one, a classical CNN directly learns from the connectivity matrices which are considered as data input instead of graphs.

A. Beta and Gamma Are Significant Bands for EEG Biometrics

Selecting proper frequency bands for EEG biometrics is important for improving performance. Therefore, we firstly evaluated our proposed method (PLV+GCNN) using EEG signals in the five canonical bands to identify the critical ones. In addition to GCNN, a conventional classifier MLP was used on the same input PLV to confirm the finding. Both dataset I and II were used in this analysis, spanning signals associated with six different human states (EO, EC, PHY, IMA, ATT, and IMG). As shown in Fig. 3, the beta and gamma bands achieved higher CRR than the other three bands, regardless of the types of classifiers or human states being used. This finding indicates that the higher frequency bands may be more closely related with human distinctiveness whereas the lower frequency bands are more related with common functions. Therefore, we selected beta and gamma bands for generating FCGs ($M = 2$) of the proposed method. Accordingly, the size of the adjacency matrix of an FCG is 128×128 in dataset I and 92×92 in dataset II. For the sake of brevity, we simply refer to 'PLV/COR in beta and gamma bands' as 'PLV/COR' in the following analysis.

B. Evaluation and Comparison

The results of each method for the three experiments are summarized in Table V, Table VI and Table VII, respectively. One-tailed paired t-test with significance levels 0.05 and 0.01 was conducted on the results of every two methods to validate whether the difference between the means of the two groups is statistically significant (See Supplementary Materials for details). Among all the methods, the proposed PLV+GCNN model consistently provided the highest CRR with EEG signals in different human states. In the first experiment, PLV+GCNN achieved an averaged CRR of 99.96% on dataset I and an averaged CRR of 98.94% on dataset II. In experiment 2, since the training and testing were performed with signals in different states, the performance of all methods was degraded, especially the methods using uni-variant features. However, PLV+GCNN was able to generalize over diverse states using abstracts learned from resting states. In experiment 3 where signals in diverse states were mixed, the PLV+GCNN model achieved an averaged CRR of 99.98% on dataset I and 98.96% on dataset II. The t-test results show that there is a statistically significant difference between the CRR means of PLV+GCNN and the comparison methods.

TABLE V

EXPERIMENT 1 – TRAINING AND TESTING WITHIN EACH HUMAN STATE. RESULTS ARE CRR IN TESTING STAGE (AVERAGE ± STANDARD DEVIATION OF 5-FOLD CROSS VALIDATION)(%)

Method	Dataset I				Dataset II			
	EO	EC	PHY	IMA	EC	EO	ATT	IMG
PLV+GCNN	99.97 ± 0.03	99.88 ± 0.03	99.99 ± 0.02	100.00 ± 0.00	98.55 ± 0.24	99.10 ± 0.13	99.25 ± 0.21	98.88 ± 0.18
COR+GCNN	99.75 ± 0.11	99.48 ± 0.26	99.94 ± 0.02	99.98 ± 0.02	98.00 ± 0.36	98.39 ± 0.49	98.99 ± 0.08	91.38 ± 6.11
PLV+CNN	99.36 ± 0.03	99.02 ± 0.04	99.41 ± 0.02	99.84 ± 0.00	98.13 ± 0.29	99.03 ± 0.06	99.18 ± 0.21	98.65 ± 0.19
COR+CNN	98.75 ± 0.14	98.13 ± 0.27	99.34 ± 0.02	99.75 ± 0.02	97.79 ± 0.38	98.42 ± 0.61	98.86 ± 0.86	91.07 ± 4.18
Raw+CNN	96.89 ± 0.77	67.43 ± 47.36	97.96 ± 1.55	97.42 ± 0.83	42.38 ± 46.53	47.58 ± 41.73	46.02 ± 42.87	20.95 ± 2.18
PLV+MLP	97.34 ± 0.54	96.14 ± 0.56	98.44 ± 0.36	98.50 ± 0.31	93.73 ± 1.40	95.32 ± 1.08	94.14 ± 0.67	93.64 ± 0.39
COR+MLP	91.29 ± 0.32	93.36 ± 0.34	96.11 ± 0.77	97.26 ± 0.49	92.40 ± 0.62	93.02 ± 0.83	87.81 ± 0.74	84.59 ± 0.89
PSD+RF	91.82 ± 0.80	89.72 ± 0.28	96.05 ± 0.21	95.79 ± 0.81	76.54 ± 1.34	82.66 ± 0.59	78.84 ± 0.93	61.86 ± 1.43
AR+SVM	89.56 ± 0.66	87.95 ± 0.49	68.41 ± 0.87	72.33 ± 0.29	72.20 ± 1.15	75.01 ± 1.23	73.14 ± 0.53	61.02 ± 1.52
FuzzEn+SVM	84.14 ± 0.83	83.73 ± 0.71	77.93 ± 0.59	80.84 ± 0.18	71.10 ± 1.29	79.19 ± 0.36	69.29 ± 0.48	61.48 ± 1.72
PSD+AR+FuzzEn+SVM	93.63 ± 0.60	91.36 ± 0.19	93.68 ± 0.30	94.30 ± 1.00	75.03 ± 1.78	82.27 ± 0.95	77.43 ± 1.80	60.14 ± 0.55
PSD+AR+FuzzEn+CNN	99.42 ± 0.39	99.57 ± 0.10	99.81 ± 0.03	99.79 ± 0.13	87.92 ± 1.79	93.90 ± 0.72	91.50 ± 0.39	59.39 ± 36.09
Wavelet+LDA [10]	96.28 ± 0.75	96.12 ± 0.35	97.37 ± 0.04	96.83 ± 0.41	78.35 ± 1.32	91.50 ± 0.48	90.50 ± 0.43	68.75 ± 2.39

TABLE VI

EXPERIMENT 2 – TRAINING ON RESTING STATES AND TESTING ON DIVERSE STATES. RESULTS ARE CRR IN TESTING STAGE (AVERAGE ± STANDARD DEVIATION OF 5 RUNS)(%)

Method	Dataset I		Dataset II	
	PHY	IMA	ATT	IMG
PLV+GCNN	85.40 ± 1.62	87.03 ± 2.53	83.66 ± 0.13	79.84 ± 0.33
COR+GCNN	86.99 ± 2.37	87.18 ± 2.86	59.65 ± 3.78	51.49 ± 2.52
PLV+CNN	80.52 ± 4.39	82.73 ± 3.35	83.72 ± 0.54	78.23 ± 0.37
COR+CNN	80.48 ± 5.02	81.46 ± 2.48	54.26 ± 4.23	43.82 ± 2.82
Raw+CNN	49.26 ± 3.85	52.51 ± 2.62	72.33 ± 2.35	48.80 ± 2.09
PLV+MLP	56.74 ± 1.32	57.12 ± 0.87	61.50 ± 1.10	47.39 ± 0.99
COR+MLP	58.87 ± 0.69	62.58 ± 1.31	42.30 ± 0.26	25.38 ± 0.15
PSD+RF	23.15 ± 0.74	22.13 ± 1.04	38.56 ± 0.50	22.57 ± 0.57
AR+SVM	13.99 ± 1.53	15.56 ± 2.00	38.43 ± 0.00	23.99 ± 0.01
FuzzEn+SVM	16.16 ± 0.01	15.61 ± 0.00	30.23 ± 0.00	18.79 ± 0.02
PSD+AR+FuzzEn+SVM	23.79 ± 0.24	22.71 ± 0.45	38.86 ± 1.17	21.88 ± 0.68
PSD+AR+FuzzEn+CNN	38.68 ± 0.40	39.71 ± 1.15	43.43 ± 6.12	25.02 ± 3.50

To evaluate the effectiveness of the functional connectivity features generated from our graph representation component, we compared the performance of the PLV features against all the alternative features (PSD, AR, FuzzEn, and a combination of them) with the same classifiers. CRR results and the corresponding t-test show that the graph representation method based on functional connectivity significantly improved the performance. For example, in experiment 2, with the same type of classifier CNN, PLV achieved a CRR of 80.52 ± 4.39, 82.73 ± 3.35, 83.72 ± 0.54, 78.23 ± 0.37 (%) using signals in PHY, IMA, ATT, and IMG state, respectively; yet, PSD+AR+FuzzEn+CNN only achieved a CRR of 38.68±0.40, 39.71 ± 1.15, 43.43 ± 6.12, and 25.02 ± 3.50 (%) using signals in the four states, respectively. Results validate our hypothesis that functional connectivity, as a bi-variate measure that captures the coupling relation of two signals, can make more effective features for EEG biometrics. Moreover, the performance of PLV was better than COR, indicating that phase synchronization measures (e.g.,PLV) can provide more robust functional connectivity estimation than time-domain measures (e.g.,COR) in detecting distinctive characteristics. Besides, the results suggest that proper classifiers need to be selected for different features.

Table VI demonstrates that the primary problem with the comparison methods is their limited learning capability to generalize over different states. For example, PSD+AR+FuzzEn+SVM achieved above 90% CRR on dataset I in experiment 1, however, the CRR dropped dramatically to around 23% in experiment 2. The proposed method PLV+GCNN, in contrast, still achieved above 85% CRR in experiment 2. This advantage comes from the functional connectivity-based graph representation component discussed above and the efficient classification model.

To evaluate the effectiveness of the classification component, we compared our GCNN model with classical CNN and three conventional classifiers, MLP, SVM, and RF using the same functional connectivity inputs. Results show that the GCNN and CNN models are able to generalize over different states. However, the conventional classifiers can hardly handle EEG signals of different states other than those used in the

TABLE VII
EXPERIMENT 3 – TRAINING ON DIVERSE STATES AND TESTING ON DIVERSE STATES. RESULTS ARE CRR IN TESTING STAGE (AVERAGE ± STANDARD DEVIATION OF 5-FOLD CROSS VALIDATION)(%)

Method	Dataset I-EO+EC+PHY+IMA		Dataset II-EC+EO+ATT+IMG	
	Results	# of epochs during training	Results	# of epochs during training
PLV+GCNN	99.98 ± 0.02	7.8 ± 0.8 (3s/epoch)	98.96 ± 0.12	13.6 ± 1.8 (3s/epoch)
COR+GCNN	99.15 ± 0.56	10.0 ± 3.1 (3s/epoch)	95.02 ± 1.65	11.0 ± 2.6 (3s/epoch)
PLV+CNN	99.79 ± 0.03	8.1 ± 0.6 (3s/epoch)	98.66 ± 0.18	12.5 ± 2.1 (3s/epoch)
COR+CNN	98.68 ± 0.62	10.5 ± 2.7 (3s/epoch)	95.17 ± 1.34	10.0 ± 2.8 (3s/epoch)
Raw+CNN	99.85 ± 0.06	17.6 ± 3.8 (8s/epoch)	98.53 ± 0.17	20.7 ± 2.9 (8s/epoch)
PLV+MLP	97.71 ± 2.25	–	92.10 ± 0.31	–
COR+MLP	94.35 ± 0.84	–	88.21 ± 1.28	–
PSD+RF	89.40 ± 0.12	–	68.14 ± 0.63	–
AR+SVM	75.62 ± 1.56	–	69.05 ± 0.62	–
FuzzEn+SVM	73.45 ± 0.10	–	66.61 ± 0.21	–
PSD+AR+FuzzEn+SVM	89.87 ± 0.34	–	66.76 ± 0.78	–
PSD+AR+FuzzEn+CNN	99.60 ± 0.11	18.0 ± 3.5 (3s/epoch)	67.29 ± 10.39	14.0 ± 3.5 (3s/epoch)

training phase. The t-test results show that the difference between the CRR results of the deep learning model and the conventional classifiers is statistically significant under the functional connectivity inputs. For example, in experiment 2, PLV+GCNN achieved a CRR of 85.40 ± 1.62, 87.03 ± 2.53, 83.66 ± 0.13, and 79.84 ± 0.33 (%) using signals in PHY, IMA, ATT, and IMG state, respectively. In comparison, MLP only achieved a CRR of 56.74 ± 1.32, 57.12 ± 0.87, 61.50 ± 1.10, and 47.39 ± 0.99 (%) using signals in the four states with the same PLV input. The comparative results in Table V, Table VI, and Table VII also indicated that GCNN was potentially a better solution to use the EEG FCGs than CNN. As each value in the connectivity matrix actually represents a weighted link between two EEG electrodes, the whole connectivity matrix naturally forms a connected graph. As a result, convolution operations at the graph level may provide a more effective way to handle EEG functional connectivity inputs than classical convolution operations on two-dimensional data matrix. In summary, the proposed learning model based on EEG graph representation and GCNN is demonstrated to be able to learn robust biometric traits from EEG signals for biometric identification in diverse human states.

Raw+CNN has been proposed in several studies as a good solution for EEG biometrics. However, our investigation shows it is very sensitive to human states and its capacity to generalize over different states is limited. Specifically, in experiment 1, Raw+CNN achieved high CRR using signals in PHY and IMA states, but only 20.95% in IMG; and in experiment 2, Raw+CNN only achieved an average CRR of 50.89% on dataset I and an average CRR of 60.57% on dataset II when handling signals of different states. The number of epochs and time used for training the GCNN and CNN in experiment 3 are also listed in Table VII. PLV+GCNN took an average of 7.8 epochs (3s/epoch) for training on dataset I and 13.6 epochs (3s/epoch) on dataset II. Raw+CNN achieved similar results as our model, but required longer time for training. Furthermore, the results in Table VI and Table VII indicated that using EEG signals of diverse states in the training stage helped improve the identification performance. This is because training a model with signals of diverse states allows the model to handle the EEG intra-person variations, therefore, helps it to better generalize over different human states.

The EEG signals used in our experiments were collected by two different signal acquisition systems: a BCI2000 system with wet sensors for dataset I, and a mobile system using dry-contact electrodes for dataset II. In general, the wet sensors provide higher signal quality than the dry sensors due to stable contact and higher signal noise ratio. However, a benefit of using dry EEG systems is that they do not require any skin preparation, therefore, is more user-friendly and suitable for real settings. A good identification method should not be easily affected by the EEG signals acquisition systems (wet sensors of dataset I and dry sensors of dataset II). From the results, we can notice that PLV+GCNN achieved good performance in both dataset I and II, however, the performance of some comparison methods degraded significantly in dataset II. For example, in experiment 1, PSD+RF achieved an average CRR of 91.82% and 89.72% using signals collected in EO and EC resting states by a wet-sensor system (dataset I), however, only 82.66% and 76.54% using signals collected in the same states by a dry-sensor system (dataset II), indicating that PSD+RF is susceptible to signal acquisition systems.

C. Effects of Window Size and Network Configurations

In this analysis, we investigate whether different window sizes will affect the identification performance and whether a deeper network could further improve the performance. The analysis was performed using dataset II and setting of experiment 3, which is training on diverse states and testing on diverse states. Deep learning approaches usually require a large sample size for data modeling during the training stage, as a result, a significant reduction in the number of training samples would affect the final result. Therefore, in our

TABLE VIII

EFFECTS OF THE WINDOW SIZE (WIN) AND THE NETWORK CONFIGURATIONS ON IDENTIFICATION PERFORMANCE. RESULTS ARE CRR IN TESTING STAGE (AVERAGE ± STANDARD DEVIATION OF 5-FOLD CROSS VALIDATION)(%). GC(#FILTERS)-GRAPH CONVOLUTION LAYER, P-GRAPH MAX-POOLING LAYER, FC-FULLY CONNECTED LAYER

Configuration	Win	Results	#epoch
GC(32)-P-GC(64)-P-FC	1s	98.96±00.12	13.6±1.8 (3s/epoch)
GC(32)-P-GC(64)-P-FC	2s	97.53±00.18	12.3±1.5 (3s/epoch)
GC(32)-P-GC(64)-P-FC	5s	95.64±00.23	11.5±2.4 (3s/epoch)
GC(32)-P-GC(64)-P-GC(64)-P-FC	1s	98.86±00.35	16.2±3.1 (3s/epoch)
GC(32)-P-GC(64)-P-GC(64)-P-FC	2s	98.57±00.57	15.8±2.7 (3s/epoch)
GC(32)-P-GC(64)-P-GC(64)-P-FC	5s	95.24±00.43	17.0±2.6 (3s/epoch)

experiments, we tried to minimize the bias caused by the number of training samples. To achieve that, we used the same forward steps for all the moving windows, despite the three window sizes. Specifically, the three moving windows in comparison are, 1 second with 0.5 second overlap (50% overlap), 2 seconds with 0.5 second overlap, and 5 seconds with 0.5 second overlap. For example, for a 60 second EEG signal, the three windows generate 119, 117, and 111 samples. For the model training in this experiment, the corresponding sample sizes for training are 33795 (window size 1s), 33417 (window size 2s), and 32285 (window size 5s) respectively, which results in slight data size reduction at the rates of 1.1% and 4.4% respectively for the two larger window sizes. Results in Table VIII indicate that a deeper architecture does not result in significant performance improvements, and larger window sizes do not bring improved performance. Contrarily, a slight degradation of the correct recognition rate is observed with larger window sizes.

D. Effect of the Number of Electrodes

To evaluate the effect of reducing the number of electrodes on the performance of the proposed method, we used three additional electrode settings: Cognionics QUICK-30 (29 electrodes), QUICK-20 (19 electrodes), and Emotiv EPOC+ (14 electrodes), as illustrated in Fig. 4. From the results, we can see that as the number of electrodes decreases, the performance of the algorithm degrades, especially when the number of electrodes is less than 20. The proposed method relies on forming a connectivity graph, which requires a sufficient number of nodes to support an effective analysis. This is particularly true in brain functional connectivity analysis [47], [48]. The graph representation module proposed in this study addresses this problem to some extent. By merging within-frequency and cross-frequency FCGs, we can extend the number of nodes and edges to obtain a richer graph representation of EEG signals. Another solution is to extend EEG dataset with limited data sources [49].

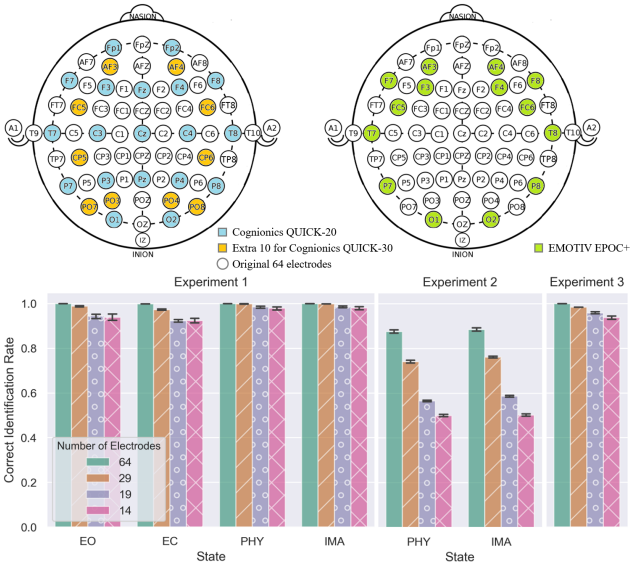

Fig. 4. Performance of proposed method (PLV+GCNN) with different electrode settings.

VI. DISCUSSION

A. Output Fusion

A moving window of one second with 50% overlap is used to generate training and testing samples. Therefore, each testing sample is based on one second EEG data and corresponds to an output which we call sample-level output. The sample-level CRR summarized in the tables shows the performance of proposed method when only one-second EEG data is used during testing phase, which can be considered as the baseline performance. When more EEG data is available during testing phase, we can fuse the outputs to further improve the performance. Fusing the outputs of multiple samples brings the system a certain fault tolerance, which could lead to better performance. Therefore, in this experiment, we generate output of each sample in a chronological order for each user during the testing phase, then apply a moving window of L length with a forward step of F to fuse the outputs. The final user identity is decided as the majority one in the window. Since sample generation is based on 1-second sliding window with 50% overlap, the data duration of a specific user required to determine his identity is $roundup(\frac{L+1}{2})$ second(s). In particular, the system degrades to sample level when $L = 1$. Fig. 5 summarizes the fusion results. It can be seen that the CRR improves with the increase of window length until convergence. This observation is consistent with our hypothesis that fusion at a higher level allows a certain fault tolerance, which leads to better performance. In practical applications, L should be properly set considering both performance and time, as too large L can seriously affect the system applicability and user experience. Empirically, L should be smaller than 10.

B. Adding New Users to the System

Adding new users to the system requires to retrain the model. Instead of training a new model from scratch, a training

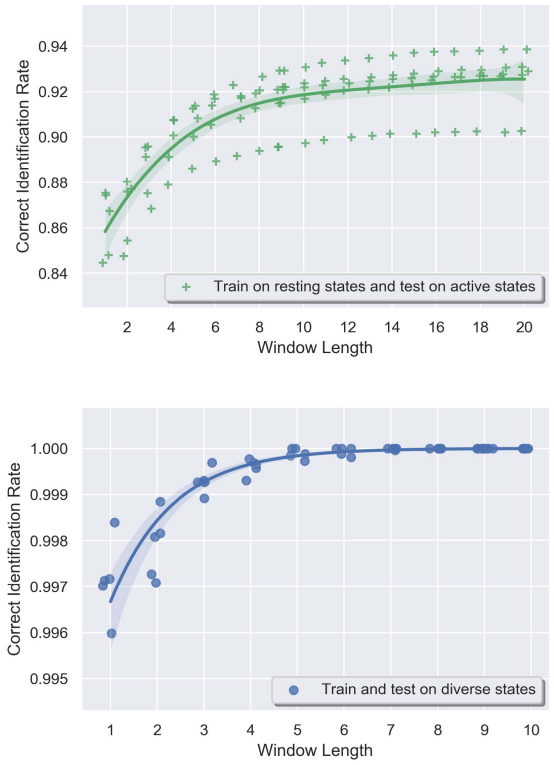

Fig. 5. Performance of output fusion.

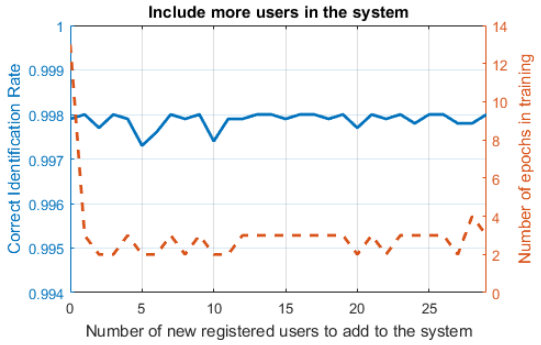

Fig. 6. Performance of adding new users to the system.

scheme based on transfer learning is proposed to tune the existing model to accommodate new users. Dataset I is used for the demonstration, which starts from 80 registered users, and shows how the network performs when accommodating one or more users into the system. The strategy is to tune the existing model trained on 80 users to transfer what have been learnt to a new model that includes more users. To make the model accommodate more users, the number of neurons in the output layer is modified to be equal to the number of users, and this is the only change to the architecture of the neural network. The evaluation procedure is summarized as the following pseudo-code. Fig. 6 shows the performance of the system when accommodating 1 to 29 new users. Both the CRR (blue curve) and the number of training epochs (red curve) are evaluated. At the starting point, generating a model for 80 users takes 13 epochs, and an average CRR of 99.79% is achieved for identifying 80 users. Then, tuning this model to accommodate an additional 1 to 29 new users takes only

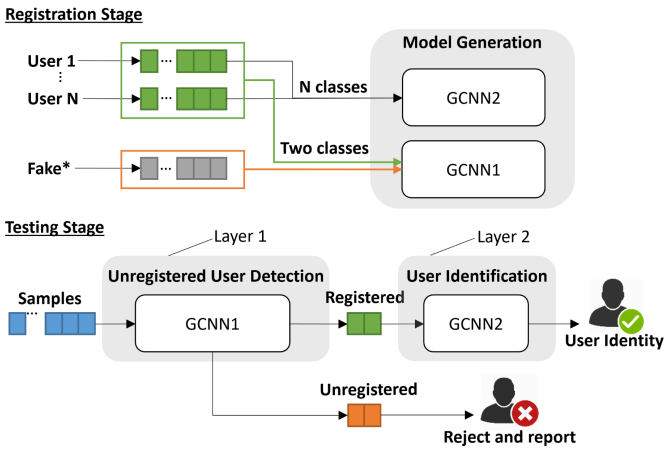

Fig. 7. Illustration of the two-layer identification system.

2 to 4 training epochs (3 seconds/epoch), significantly reducing the time required for training. The reason why tuning the model saves time is relevant to the ability of GCNN to use information extracted by the convolution layers. Usually, there is no need to extract a completely new set of features for each new user. Meanwhile, the CRR remains stable despite some slight fluctuations at $i = 5$ and $i = 10$. An average CRR of 99.81% is achieved for identifying 109 users in the end, which is not degraded compared with identifying 80 users at the starting point.

Generating original model
Training data set (80 users)
Create model ($OutputLayer = 80$)
Train and save the weights W_0

Transfer learning to accommodate one or more users
For $i = 1$, âŁ¦, 29
Update training data set ($80 + i$ users)
Load model and weights W_0
Remove the output layer and corresponding weights
Create a new output layer ($OutputLayer = 80 + i$)
Append the new output layer to the truncated model
Tune the model
Save the new model for testing

C. Rejecting Unregistered Subjects

A practical identification system should be able to correctly identify registered users and also to appropriately reject unregistered subjects, where the latter issue has been neglected in existing literature of EEG person identification system. To address this problem, a two-layer system is proposed, as illustrated in Fig 7, where each layer is itself a neural network. During the registration stage, EEG data are collected from the N users to be registered, corresponding samples are generated and labeled with the user IDs accordingly. A classification model GCNN2 is then trained using these labeled samples for identifying registered users in the second layer. Meanwhile, another classifier GCNN1 is generated for detecting unregistered users in the first layer. This classifier is trained with two classes of data: the user class which consists

TABLE IX
REJECTING UNREGISTERED USERS (FAR)(%)

EO	EC	PHY	IMA	Mixed
3.20 ± 0.59	4.49 ± 0.35	0.20 ± 0.13	0.56 ± 0.40	1.65 ± 0.39

of data from the N registered users and the unauthorized class which contains EEG data from subjects other than the N users. It is worth noting that the unauthorized data can be gathered from available datasets or online public datasets. These data are only used for training GCNN1 to force the network to learn the boundary between the N registered users and non-registered ones. During the test stage, the system will first use GCNN1 to identify whether the samples are from registered users, and if so, use GCNN2 to identify who the samples belong to. Alternatively, if unregistered samples are detected, user access will be denied and reported.

We tested the two-layer identification scheme using dataset I, where the 109 subjects were divided into three groups: (1) user group-80 subjects, (2) unauthorized group-9 subjects, and (3) impostor group-20 subjects. The user group was further divided into a training set and a testing set, where the training set contains 80% of data for each of the 80 users and the testing set contains the remaining 20% of the data in a 5-fold cross validation manner. The GCNN1 was trained using data from the user group (training section) and unauthorized group, and tested on user group (testing section) and impostor group. This partition ensures that the classifier will not see any impostor instances during the training phase; therefore, it is able to generalize to detect unauthorized access from users that were not known at the training phase. Table IX summarizes the false-acceptance rate (FAR), which measures the likelihood that the instances of unregistered users are incorrectly accepted as registered users, achieved by the first layer of the system using EEG data of four states and a mix of the four, respectively. We run each experiment 5 times and the results shown in the table are average ± standard deviation of FARs of the five runs.

VII. CONCLUSION AND FUTURE WORK

In this study, we proposed a novel model for EEG-based person identification. The model consists of two components: a graph representation component based on functional connectivity to obtain rich graph representation of EEG signals; and a classification component based on GCNN to learn discriminative structural patterns from the EEG graphs. The functional connectivity between pairs of EEG signals naturally form a graph (network), the approach proposed in this work will not sabotage the intrinsic structural relationship, but use it effectively for learning individual distinctiveness. Extensive comparisons were conducted in three experiments. The results demonstrated that the proposed method is effective and robust against different human states.

In the future study, we will extend the design to fit the authentication and continuous authentication scenarios. As industries (e.g., IBM research) emphasized that the future of identity and access management must be rooted in continuous authentication [50], there is a trend that biological signals, especially EEG, will gain growing interest. Moreover, the stability issue and permanence issue are two critical problems and challenges for EEG biometrics, in which the stability refers to the robustness against human states, and the permanence refers to the reproducibility when using EEG signals collected in different sessions. This study addresses the stability issue by investigating the robustness of each method to diverse human states. However, due to the limitation of available databases and data collection, EEG signals of single sessions were used in the analysis. Further study on the permanence issue using EEG signals collected during multiple sessions is needed. In our future work, we will extend our investigation in multi-session settings.

ACKNOWLEDGEMENT

The experiments for Dataset II were approved by the Human Research Ethics Advisory Panel of UNSW, Approval HC17434.

REFERENCES

[1] H. A. Abbass, J. Tang, R. Amin, M. Ellejmi, and S. Kirby, "Augmented cognition using real-time EEG-based adaptive strategies for air traffic control," in *Proc. Hum. Factors Ergonom. Soc. Annu. Meeting*, vol. 58. Los Angeles, CA, USA: SAGE, no. 1, 2014, pp. 230–234.
[2] D. Tan and A. Nijholt, "Brain-computer interfaces and human-computer interaction," in *Brain-Computer Interfaces*. London, U.K.: Springer, 2010, pp. 3–19.
[3] B. K. Min, M. J. Marzelli, and S. S. Yoo, "Neuroimaging-based approaches in the brain-computer interface," *Trends Biotechnol.*, vol. 28, pp. 552–560, Nov. 2010.
[4] P. Campisi and D. La Rocca, "Brain waves for automatic biometric-based user recognition," *IEEE Trans. Inf. Forensics Security*, vol. 9, no. 5, pp. 782–800, May 2014.
[5] M. Wang, H. A. Abbass, and J. Hu, "EEG-based biometrics for person identification and continuous authentication," in *Information Security: Foundations, Technologies and Applications*, A. I. Awad and M. Fairhurst, Eds. Edison, NJ, USA: IET, 2018, ch. 13.
[6] J. A. Unar, W. C. Seng, and A. Abbasi, "A review of biometric technology along with trends and prospects," *Pattern Recognit.*, vol. 47, no. 8, pp. 2673–2688, 2014.
[7] M. V. Ruiz-blondet, Z. Jin, and S. Laszlo, "CEREBRE: A novel method for very high accuracy event-related potential biometric identification," *IEEE Trans. Inf. Forensics Security*, vol. 11, no. 7, pp. 1618–1629, Jul. 2016.
[8] B.-K. Min, H.-I. Suk, M.-H. Ahn, M.-H. Lee, and S.-W. Lee, "Individual identification using cognitive electroencephalographic neurodynamics," *IEEE Trans. Inf. Forensics Security*, vol. 12, no. 9, pp. 2159–2167, Sep. 2017.
[9] D. La Rocca *et al.*, "Human brain distinctiveness based on EEG spectral coherence connectivity," *IEEE Trans. Biomed. Eng.*, vol. 61, no. 9, pp. 2406–2412, Sep. 2014.
[10] S. Yang, F. Deravi, and S. Hoque, "Task sensitivity in EEG biometric recognition," *Pattern Anal. Appl.*, vol. 21, no. 1, pp. 105–117, 2018.
[11] E. Maiorana, D. La Rocca, and P. Campisi, "On the permanence of EEG signals for biometric recognition," *IEEE Trans. Inf. Forensics Security*, vol. 11, no. 1, pp. 163–175, Jan. 2016.
[12] B. C. Armstrong, M. V. Ruiz-Blondet, N. Khalifian, K. J. Kurtz, Z. Jin, and S. Laszlo, "Brainprint: Assessing the uniqueness, collectability, and permanence of a novel method for ERP biometrics," *Neurocomputing*, vol. 166, pp. 59–67, Oct. 2015.
[13] C. N. Gupta, R. Palaniappan, and R. Paramesran, "Exploiting the P300 paradigm for cognitive biometrics," *Int. J. Cognit. Biometrics*, vol. 1, no. 1, pp. 26–38, 2012.
[14] R. Palaniappan and D. P. Mandic, "Biometrics from brain electrical activity: A machine learning approach," *IEEE Trans. Pattern Anal. Mach. Intell.*, vol. 29, no. 4, pp. 738–742, Apr. 2007.
[15] R. Das, E. Maiorana, and P. Campisi, "EEG biometrics using visual stimuli: A longitudinal study," *IEEE Sign. Process. Lett.*, vol. 23, no. 3, pp. 341–345, Mar. 2016.

[16] A. Riera, A. Soria-Frisch, M. Caparrini, C. Grau, and G. Ruffini, "Unobtrusive biometric system based on electroencephalogram analysis," *EURASIP J. Adv. Signal Process.*, vol. 2008, no. 18, pp. 1–8, 2008.
[17] P. Campisi *et al.*, "Brain waves based user recognition using the 'eyes closed resting conditions' protocol," in *Proc. IEEE Int. Workshop Inf. Forensics Security*, Nov./Dec. 2011, pp. 1–6.
[18] D. La Rocca, P. Campisi, and G. Scarano, "On the repeatability of EEG features in a biometric recognition framework using a resting state protocol," in *Proc. BIOSIGNALS*, 2013, pp. 419–428.
[19] S. Yang and F. Deravi, "On the usability of electroencephalographic signals for biometric recognition: A survey," *IEEE Trans. Human-Mach. Syst.*, vol. 47, no. 6, pp. 958–969, Dec. 2017.
[20] R. Palaniappan, "Two-stage biometric authentication method using thought activity brain waves," *Int. J. Neural Syst.*, vol. 18, no. 1, pp. 59–66, 2008.
[21] S. Marcel and J. D. R. Millán, "Person authentication using brainwaves (EEG) and maximum *a posteriori* model adaptation," *IEEE Trans. Pattern Anal. Mach. Intell.*, vol. 29, no. 4, pp. 743–752, Apr. 2007.
[22] Z. Mu, J. Hu, and J. Min, "EEG-based person authentication using a fuzzy entropy-related approach with two electrodes," *Entropy*, vol. 18, no. 12, p. 432, 2016.
[23] S. Yang and F. Deravi, "Novel HHT-based features for biometric identification using EEG signals," in *Proc. 22nd Int. Conf. Pattern Recognit. (ICPR)*, Aug. 2014, pp. 1922–1927.
[24] B. Platt and G. Riedel, "The cholinergic system, EEG and sleep," *Behavioural Brain Res.*, vol. 221, no. 2, pp. 499–504, 2011.
[25] T. C. Ferree, P. Luu, G. S. Russell, and D. M. Tucker, "Scalp electrode impedance, infection risk, and EEG data quality," *Clin. Neurophysiol.*, vol. 112, no. 3, pp. 536–544, 2001.
[26] M. Fraschini, A. Hillebrand, M. Demuru, L. Didaci, and G. L. Marcialis, "An EEG-based biometric system using eigenvector centrality in resting state brain networks," *IEEE Signal Process. Lett.*, vol. 22, no. 6, pp. 666–670, Jun. 2015.
[27] W. Kong, Q. Fan, L. Wang, B. Jiang, Y. Peng, and Y. Zhang, "Task-free brainprint recognition based on degree of brain networks," in *Proc. Int. Conf. Neural Inf. Process.* Cham, Switzerland: Springer, 2017, pp. 709–717.
[28] H. Cecotti and A. Graser, "Convolutional neural networks for P300 detection with application to brain-computer interfaces," *IEEE Trans. Pattern Anal. Mach. Intell.*, vol. 33, no. 3, pp. 433–445, Mar. 2011.
[29] M. Wang, S. Abdelfattah, N. MoustafaNour, and J. Hu, "Deep Gaussian mixture-hidden Markov model for classification of EEG signals," *IEEE Trans. Emerg. Topics Comput. Intell.*, vol. 2, no. 4, pp. 278–287, Aug. 2018.
[30] R. Das, E. Maiorana, and P. Campisi, "Visually evoked potential for EEG biometrics using convolutional neural network," in *Proc. 25th Eur. Signal Process. Conf. (EUSIPCO)*, Aug./Sep. 2017, pp. 951–955.
[31] H. El-Fiqi, M. Wang, N. Salimi, K. Kasmarik, M. Barlow, and H. Abbass, "Convolution neural networks for person identification and verification using steady state visual evoked potential," in *Proc. IEEE Int. Conf. Syst., Man, Cybern. (SMC)*, Oct. 2018, pp. 1062–1069.
[32] Z. Mao, W. X. Yao, and Y. Huang, "EEG-based biometric identification with deep learning," in *Proc. 8th Int. IEEE/EMBS Conf. Neural Eng. (NER)*, May 2017, pp. 609–612.
[33] L. Chu, R. Qiu, H. Liu, Z. Ling, T. Zhang, and J. Wang. (2017). "Individual recognition in schizophrenia using deep learning methods with random forest and voting classifiers: Insights from resting state EEG streams." [Online]. Available: https://arxiv.org/abs/1707.03467
[34] L. Ma, J. W. Minett, T. Blu, and W. S.-Y. Wang, "Resting state EEG-based biometrics for individual identification using convolutional neural networks," in *Proc. 37th Annu. Int. Conf. Eng. Med. Biol. Soc. (EMBC)*, Aug. 2015, pp. 2848–2851.
[35] Q. Gui, W. Yang, M. V. Ruiz-Blondet, S. Laszlo, and Z. Jin, "An unsupervised, EEG-based person identification approach using convolutional neural networks," in *Proc. 42nd Annu. Northeast Bioeng. Conf. (NEBEC)*, 2016, pp. 1–2.
[36] T. Schons, G. J. P. Moreira, P. H. L. Silva, V. N. Coelho, and E. J. S. Luz, "Convolutional network for EEG-based biometric," in *Proc. Iberoamerican Congr. Pattern Recognit.* Cham, Switzerland: Springer, 2017, pp. 601–608.
[37] Q. Wu, Y. Zeng, C. Zhang, L. Tong, and B. Yan, "An EEG-based person authentication system with open-set capability combining eye blinking signals," *Sensors*, vol. 18, no. 2, p. 335, 2018.
[38] M. Defferrard, X. Bresson, and P. Vandergheynst, "Convolutional neural networks on graphs with fast localized spectral filtering," in *Proc. Adv. Neural Inf. Process. Syst.*, 2016, pp. 3844–3852.
[39] F. Varela, J.-P. Lachaux, E. Rodriguez, and J. Martinerie, "The brainweb: Phase synchronization and large-scale integration," *Nature Rev. Neurosci.*, vol. 2, no. 4, pp. 229–239, 2001.
[40] T. N. Kipf and M. Welling. (2016). "Semi-supervised classification with graph convolutional networks." [Online]. Available: https://arxiv.org/abs/1609.02907
[41] D. P. Kingma and J. Ba, "Adam: A method for stochastic optimization," in *Proc. 3rd Int. Conf. Learn. Represent. (ICLR)*, 2015, pp. 1–15.
[42] S. Ioffe and C. Szegedy. (2015). "Batch normalization: Accelerating deep network training by reducing internal covariate shift." [Online]. Available: https://arxiv.org/abs/1502.03167
[43] N. Srivastava, G. Hinton, A. Krizhevsky, I. Sutskever, and R. Salakhutdinov, "Dropout: A simple way to prevent neural networks from overfitting," *J. Mach. Learn. Res.*, vol. 15, no. 1, pp. 1929–1958, 2014.
[44] A. L. Goldberger *et al.*, "Physiobank, physiotoolkit, and physionet: Components of a new research resource for complex physiologic signals," *Circulation*, vol. 101, no. 23, pp. e215–e220, 2000.
[45] G. Schalk, D. J. McFarland, T. Hinterberger, N. Birbaumer, and J. R. Wolpaw, "BCI2000: A general-purpose brain-computer interface (BCI) system," *IEEE Trans. Biomed. Eng.*, vol. 51, no. 6, pp. 1034–1043, Jun. 2004.
[46] I. Winkler, S. Brandl, F. Horn, E. Waldburger, C. Allefeld, and M. Tangermann, "Robust artifactual independent component classification for BCI practitioners," *J. Neural Eng.*, vol. 11, no. 3, 2014, Art. no. 035013.
[47] E. S. Finn *et al.*, "Functional connectome fingerprinting: Identifying individuals using patterns of brain connectivity," *Nature Neurosci.*, vol. 18, no. 11, pp. 1664–1671, 2015.
[48] C. M. Michel and M. M. Murray, "Towards the utilization of EEG as a brain imaging tool," *Neuroimage*, vol. 61, no. 2, pp. 371–385, 2012.
[49] S. M. Abdelfattah, G. M. Abdelrahman, and M. Wang, "Augmenting the size of EEG datasets using generative adversarial networks," in *Proc. Int. Joint Conf. Neural Netw. (IJCNN)*, Jun. 2018, pp. 1–6.
[50] G. Wu, J. Wang, Y. Zhang, and S. Jiang, "A continuous identity authentication scheme based on physiological and behavioral characteristics," *Sensors*, vol. 18, no. 1, p. 179, 2018.

Min Wang is currently pursuing the Ph.D. degree in computer science from the School of Engineering and Information Technology, University of New South Wales, Canberra, Australia. Her research interests include pattern recognition, signal processing, deep learning, and human–machine interaction.

Heba El-Fiqi received the B.Sc. degree in computer science from Zagazig University, Egypt, in 2003, the M.Sc. degree in computer science from Cairo University, Egypt, in 2008, and the Ph.D. degree in computer science from the University of New South Wales (UNSW), Canberra, Australia, in 2013. She is currently a Post-Doctoral Research Associate with the Trusted Autonomy Research Group, UNSW. Her research interests include machine learning, trusted autonomous systems, artificial intelligence, computational linguistics, computer networks, and security systems.

Jiankun Hu is currently a Full Professor of cybersecurity with the School of Engineering and IT, University of New South Wales, Canberra, Australia. His main research interest is in the field of cybersecurity, including biometrics security, where he has publications at top venues, including the IEEE TRANSACTIONS ON PATTERN ANALYSIS AND MACHINE INTELLIGENCE. He has served on the editorial boards of up to seven international journals, including the IEEE TRANSACTIONS ON INFORMATION FORENSICS AND SECURITY.

Hussein A. Abbass (SM'05) is currently a Professor of information technology with the University of New South Wales, Canberra, Australia. His main research interest is in artificial intelligence, brain–computer interfaces, and swarm intelligence. He is a fellow of the Australian Computer Society, the Operational Research Society, and the Australian Institute of Management. He has been the Vice President for Technical Activities for the IEEE Computational Intelligence Society since 2016 and the National President for the Australian Society of Operations Research from 2016 to 2019. He is an Associate Editor of the IEEE TRANSACTIONS ON EVOLUTIONARY COMPUTATION, the IEEE TRANSACTIONS ON CYBERNETICS, the IEEE TRANSACTIONS ON COGNITIVE AND DEVELOPMENTAL SYSTEMS, the IEEE TRANSACTIONS ON COMPUTATIONAL SOCIAL SYSTEMS, and four other journals.